Wisconsin
Indiana
Yale
Noao

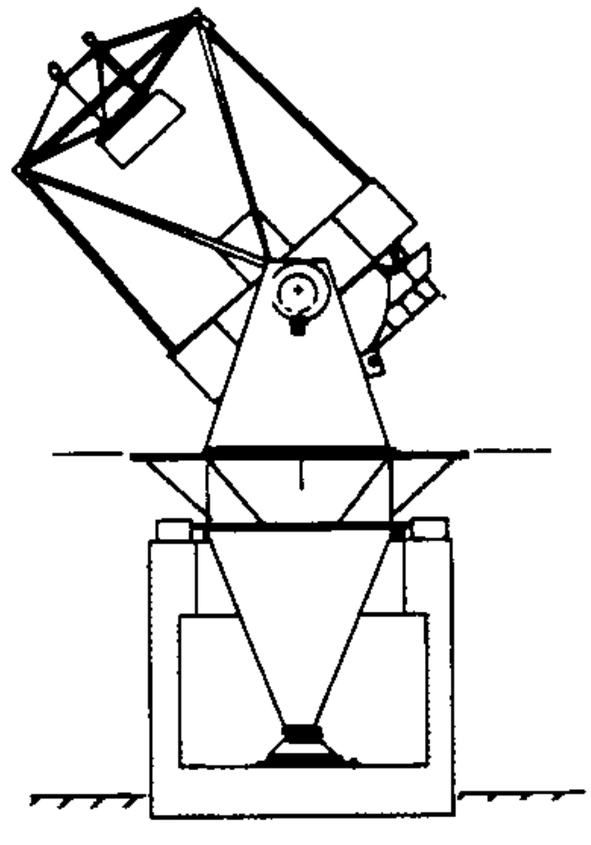

3.5 Meter Telescope

Stress at the Support Interface of a 3.5m Borosilicate Honeycomb Mirror

W.-Y. Wong

WODC 02-18-01

April 30, 1990

Stress at the support interface of a 3.5m borosilicate honeycomb mirror

Woon-Yin Wong
Kitt Peak National Observatory
Tucson, AZ 85726-6732

April 30, 1990

Abstract

Two investigations on the stress level around the mirror supporting area were made. One was on the mirror's self-weight stress in a 3-point-support system. The other was on the stress level of the mirror with a 66-point active-support system with one of the supports exerting a maximum force of 250-lb. normal to the back. It was found that the stress levels for both cases are below the adopted limiting tensile stress level of 725 psi with a large safety margin. The tensile stress for the first case is found to be 182 psi with a safety factor of 4. The maximum absolute stress value for the second case (since the 250-lb. force can be applied in either push or pull) is found to be 79 psi with a safety factor of 9.

Introduction

Two questions have been raised about the support of the 3.5m mirror: First, what is the stress level within the mirror when being supported at 3 points (Figure 1a)? And second, what is the stress level when one of the 66 active supports produces a most demanding correction, i.e., 250 pounds of push or pull (Figure 1b)? The former question applies to cases during mirror handling, such as when the thermal sensors are installed, or the mirror is being transported; and the latter for future normal operation.

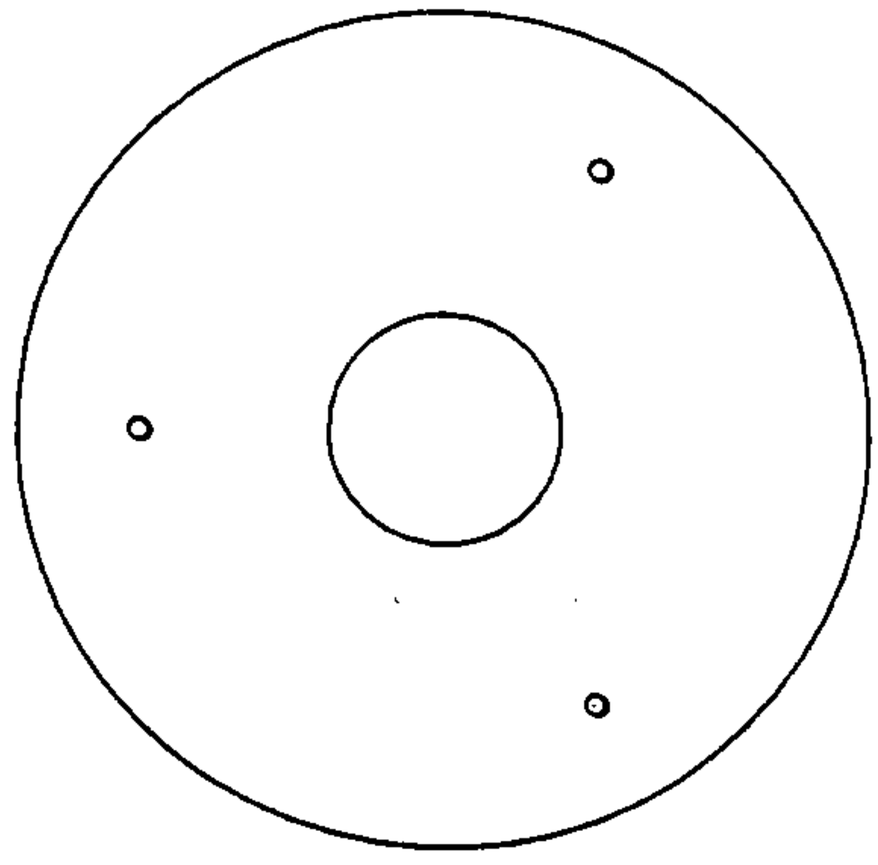

(a)

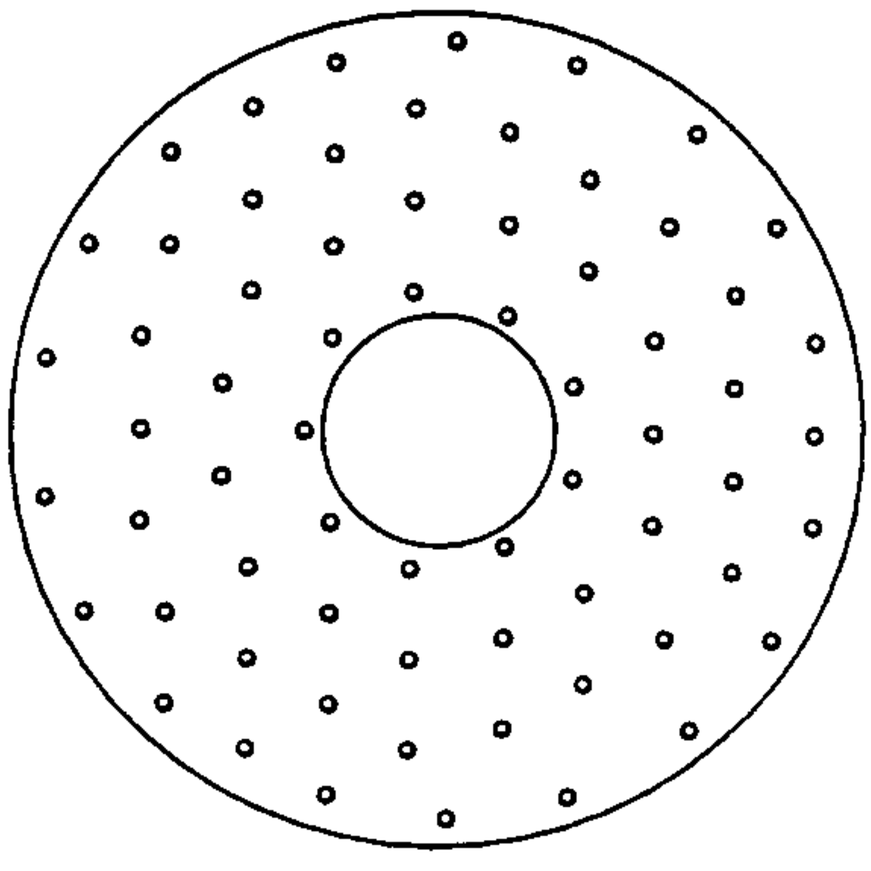

(b)

Figure 1. Two loading conditions are investigated. (a) To study the stress caused by the mirror's own weight when supported at 3 locations. (b) To study the stress when the mirror is supported at 66 points, with one support force reaching its limit of 250 lbs.

Usually the primary concern of mirror analyses is surface distortion. Stress levels are usually low when the mirror is supported by a well designed support system. Numerous mirror studies on surface error have been made on various projects, such as the Texas 300-inch mirror study [1], NNTT and ESO 8-m mirror studies [2,3], the 120-inch mirror study for the Charles Stark Draper Laboratory, Inc. [4], and the British large telescope project [5]. In all cases stress levels within the mirror are low because the mirror is not subjected to any survival environments.

However, understanding the internal stress level during operations other than observation, when the mirror is supported by a less sophisticated system such as a simple kinematic mount, is equally important. The concern is whether the mirror is subjected to damage due to high stress concentration. Handling of 8m class thin mirrors has been examined by ESO's VLT group [3]. The max. stress in their study was found to be about 25% below the recommended stress value when the blank is supported at three points.

More importantly, since the mirror will also be subjected to forced distortion during normal observing conditions, even though the excursion is at sub-wavelength level, the understanding of the relation between stress and strain will be particularly useful.

This report includes the study of stress level on a global model, comparing the results using two different types of finite elements (one with the bending stiffness and the other without); and the studies of stress level on a detailed local model. Global model analyses show a general picture of stress distribution whereas the local model study shows a detailed picture of stress distribution. The former study also provides information which was subsequently used as boundary conditions to the latter studies.

Global model

The element types

A model using type-6 elements was prepared by W. Keppel in 1989 [6]. The model has 994 nodes and 12 element groups. It has three supports 120 degrees apart in a circle with a radius of 48 inches. An analysis on the gravity effect was made. The surface distortion is shown in Figure 2(a) with both tilting and focusing adjustments made.

The SAP-IV type-6 element [7] is a quadrilateral plate and shell element. It contains 3 or 4 nodes (5 nodes in case of a curved surface but was never used in this model). The stress computation provides the membrance stress σ_{x1} and σ_{y1}, moments per unit length normal to the membrance M_x, M_y, and shear τ_{xy}. The stress distribution along the depth of the element is not

computed. Therefore the skin stress caused by the bending moments are needed to be further evaluated. The basic formulae to determine the principal stress and the additional stress due to bending at a given distance h/2 from the neutral plane are shown below.

Membrane stress from the SAP-IV computation:

σ_{x1} in x-direction

σ_{y1} in y-direction (1)

Pure bending stress from a bending moment M at a distance h from the neutral-plane of the element:

$$\sigma_{x2} = \frac{6}{h^2} M_x$$

$$\sigma_{y2} = \frac{6}{h^2} M_y \qquad (2)$$

Then the stress on the surface of the element is a combination of expression (1) and (2):

in x-direction: $\sigma_x = \sigma_{x1} + \sigma_{x2}$

in y-direction: $\sigma_y = \sigma_{y1} + \sigma_{y2}$ (3)

Consequently, the shear stress in each element is

$$\text{Shear} \quad \tau = \sqrt{\frac{1}{4}(\sigma_x - \sigma_y)^2 + \tau_{xy}} \qquad (4)$$

And the principal stress is

$$\sigma_{max/min} = \frac{1}{2}(\sigma_x + \sigma_y) \pm \tau \ . \qquad (5)$$

The SAP-IV type-3 element is a plane stress membrane element. Bending moments are not considered in the computation. Values in eq. (2) are all equal to zero. One analysis using type-3 elements was made to investigate if bending stress does play an important role when the mirror is supported by a 3-point system. The result is shown in figure 2(b). Further discussions are made in the next section.

The bending effect

Two analyses, one with type-6 elements including the bending stiffness, and another with type-3 elements considering only the in-plane strength were made. Their results showed that the bending moment effect is low. It is illustrated in Figure 2 as well as by those parameters summarized in Table I.

Table I. Analytical results using two different types of element

	type-6	type-3
peak to valley (wave)	14.2	14.8
avg. disp. of surface (micro-in.)	1.48	1.49
rms dev. from the avg. (micro-in.)	76.84	78.66

The maximum, minimum principal stresses and shear stress from both type-3 and type-6 element analyses are listed in Table II. Only the peak values in each of the 12 element groups are listed. When the bending effect is taken into account, the maximum principal stress is 42 psi, the minimum principal stress 247 psi, and the shear 142 psi. By using type-3 elements, the result is slightly pessimistic, with the maximum stress at 50 psi, minimum stress at 278 psi, and shear at 164 psi. The differences are 19% in tension, 13% in compression and 15% in shear. The highest stress is located at the rib immediately above the support.

Table II. Stress with the mirror supported at 3 points - from the global model No bending effect in type-3 (t-3) element, with bending in type-6 (t-6) element.

			Principal stresses					
			max. (psi)		min. (psi)		shear (psi)	
group	elem. no.	t(in.)	t-3	t-6	t-3	t-6	t-3	t-6
1	149	1.75	14	32	-6	-8	6	10
2	136	1.75	14	29	-6	-8	6	4
3	149	.64	13	20	-43	-43	12	27
4	136	.64	13	17	-43	-63	12	20
5	206	.44	46	40	-58	-57	49	49
6	200	.44	46	40	-58	-58	49	49
7	206	.44	50	42	-278	-247	164	142
8	200	.44	50	39	-278	-247	164	141
9	45	.50	11	11	-10	-10	10	10
10	45	.50	10	10	-12	-14	10	10
11	15	.50	5	4	-4	-3	3	2
12	15	.50	6	7	-6	-7	3	3

Note : groups 1 and 2 represent the front plate, group 3 and 4 the back plate, 5 and 6 the upper half rib, 7 and 8 the lower half rib, 9 and 10 the outer ring, 11 and 12 the inner ring. The thickness of the front face plate is as cast. The final dimension will be 1.2 inches. The back face plate is 1 inch thick. The dimension shown of .64 inch represents the reduction of stiffness due to the opening in the center.

Histograms summarizing the stress distribution are illustrated in Figure 3. It is another indication showing the similarity of these two analytical approaches for this particular case. The similarity of these results implies that using type-6 element, together with the formulae listed in eq. (1) thru (5), for the detailed local model might be sufficient. However, as was shown later, the local model was constructed with type-5 brick elements. While it requires more computational effort for the problem, it is a more precise approach.

Local Models

Description of model

The type-5 element in SAP-IV is a three dimensional solid element consists of eight nodes. It is an isoparametric element, each node has three translational degrees of freedom. Six stress components and three principal stresses are computed at the center of each element surface.

Figure 4 shows the locations of these two local models within the global model. Each model covers the lower half of one and one-half cells. Except for the absence of through holes on the ribs, the model is an exact replication of the mirror part. The coordinate system used for the models are the same as the global model. The 3-point-support model and the 66-point-support model are different because of different support locations. Each model has its own coordinate system and boundary condition. The control coordinates of the two systems are listed in Table III, and the boundary conditions are listed in Table IV. The geometry of these type-5 brick elements are illustrated in Figure 5. The relevant parameters about the model are as follows:

Total node number is 853.

There are 6 groups of type-5 elements:

group 1 : 60 elements representing the 1 in. back plate in the half cell.
group 2 : 120 elements representing the 1 in. back plate in the whole cell.
group 3 : 100 elements representing the 1/4 in. ribs in the half cell.
group 4 : 200 elements representing the 1/4 in. ribs in the whole cell.
group 5 : 10 elements representing the fillet in the half cell.
group 6 : 20 elements representing the fillet in the whole cell.

and 3 groups of type-7 elements:

group 7 : 156 elements representing the boundary conditions in x direction.
group 8 : 252 elements representing the boundary conditions in y direction.
group 9 : 156 elements representing the boundary conditions in z direction.

Later, two more groups are added to the model:

group 10 : 15 elements representing the invar pad
group 11 : 8 elements representing the 1.5 inch hole on the rib with 4 elements deleted in group 4.

The numbering for the local model is partially shown in Figure 6. The numbers are generated by a series of programs (coor.f, pt.f, and touchup.f), and the listings are included in Appendix A for reference. An additional program listing for the generation of boundary conditions by linear interpretation (typ702.f) is also included in the appendix.

Table III. Nodal coordinate systems used in the two local models, one for the 3-pt. support, and another for the 66-pt. support. Units in inches.

local node	3-pt supp global node	x	y	z	66-pt supp global node	x	y	z
220	47	56.74	0.00	7.76	128	43.65	0.00	7.08
210	48	56.74	0.00	0.00	129	43.65	0.00	0.00
222	50	54.56	3.78	7.64	131	41.47	3.78	6.99
232	51	54.56	3.78	0.00	132	41.47	3.78	0.00
330	83	48.01	0.00	7.28	176	34.92	0.00	6.72
320	84	48.01	0.00	0.00	177	34.92	0.00	0.00
264	86	50.19	3.78	7.40	179	37.10	3.78	6.81
254	87	50.19	3.78	0.00	180	37.10	3.78	0.00
462	89	48.01	7.56	7.31	182	34.92	7.56	6.75
452	90	48.01	7.56	0.00	183	34.92	7.56	0.00
396	128	43.65	0.00	7.05	227	30.55	0.00	6.57
386	129	43.65	0.00	0.00	228	30.55	0.00	0.00
418	131	41.47	3.78	6.99	230	28.37	3.78	6.51
408	132	41.47	3.78	0.00	231	28.37	3.78	0.00
440	134	43.65	7.56	7.10	233	30.55	7.56	6.60
430	135	43.65	7.56	0.00	234	30.55	7.56	0.00

The boundary conditions for the local models are based on the analytical results of the global model. The nodal displacements of those control nodes at the boundary (from type-6 analysis) are listed in Table IV below. These values are used as 'support-displacements' in the type-7 boundary elements used in the local model.

Table IV. Nodal displacements from type-6 element analysis defining the local model boundaries. Unit for dx dy dz are in micro-inch.

	3-point support				66-point support			
node(local)	node(global)	dx	dy	dz	node(global)	dx	dy	dz
220	47	64	0	-99	128	3	0	24
210	48	42	0	-100	129	-1	0	24
222	50	70	0	-85	131	6	1	28
232	51	39	-10	-85	132	-1	-1	28
330	83	54	0	7	176	1	0	59
320	84	46	0	234	177	2	0	127
264	86	71	23	-35	179	6	8	44
254	87	43	-14	-9	180	0	-3	51
462	89	51	9	-82	182	0	4	29
452	90	47	-21	-84	183	2	-4	28
396	128	26	0	-22	227	-8	0	45
386	129	56	0	0	228	6	0	51
418	131	47	9	-67	230	-1	3	30
408	132	52	-12	-68	231	5	-2	29
440	134	55	0	-89	233	1	1	25
430	135	50	-17	-89	234	3	-3	25

The directory for the type-5 element numbering system is useful because of the cross-reference to the stress output. It is included in Appendix B for reference.

The numbering of the node points allows convenience in the model making, but does not minimize the computational effort. For the size of this model, a re-numbering procedure is necessary and indispensable. The computation takes approximately 30 minutes for each analysis. Without the re-numbering procedure, the stiffness matrix bandwidth will become so large that the computation will not be successful.

Stress under its own weight at 3-point support without pad or hole on rib

The analysis was first made without a supporting invar pad (2.5 in. in diameter) or a hole (1.5 in. in diameter) in the rib. The influence force and the adjustment used in the analysis are listed in eq. (6).

$$\begin{aligned} &1361 \text{ lb.} && \text{(used in the analysis)} \\ &4427 \text{ lb.} / 3 = 1476 \text{ lb.} && \text{(realistic value)} \\ &1467 / 1361 = 1.084 && \text{(adjustment)} \end{aligned} \tag{6}$$

The applied force is transmitted through an area covered by the supporting pad which consists of 40 nodes (6 on the boundary and 17 on each side of the plane of symmetry). It is assumed that the force is equally divided by those nodes (at boundary : 85, 199, 320, 331, 342, 353; outside of boundary : 81, 166, 177, 188, 287, 298, 309, 507, 518, 529, 540, 551, 562, 573, 714, 718, 722). Each node takes 34 lbs. of force. The summary of the analytical result (Dsap4.pre11), in terms of maximum and minimum principal stresses is listed below in Table V. These values represent the stress at the exposed surface. The remaining internal stresses are not being examined.

Table V. Max. & min. principal stresses at the exposed surface of the detail model (no supporting pad or hole on rib).

group	max. (psi)		min. (psi)	
	computed	adjusted	computed	adjusted
1	89.	97.	-360.	-390.
2	92.	100.	-350.	-380.
3	61.	66.	-307.	-332.
4	61.	66.	-306.	-332.
5	106.	115.	-176.	-191.
6	115.	125.	-171.	-185.

And the peak stress values are:

$$\begin{aligned} &\text{max. principal stress} = 125 \text{ psi} \\ &\text{min. principal stress} = -390 \text{ psi} \end{aligned} \tag{7}$$

Stress under its own weight for 3-point support with a pad and a hole in the rib

The assumption that the reactive force at each support is equally divided over the 40 nodes within a 2.5-inch diameter supporting pad area is not entirely correct. To ensure the analytical model is closer to the real case, an additional model representing the pad is added. An engineering drawing of the pad is illustrated in Figure 7b. The load, as shown in eq. (6), and its computed reaction, are illustrated in Figure 7a. The analytical result (Dsap4.pad01) showed that the reactive force concentrates mainly at the stem area, only a small amount of force is spread out to the rim of the pad. (One attempt to make the reactive force more uniform by adding gusset plates between the stem and the pad failed to redistribute the reaction significantly).

A 1.5-inch through hole on one rib was also added to the model to investigate the possible stress concentration around that area. The hole location, however, does not represent the true geometry due to the limitation in this local model. The nominal distance between the hole and the back plate is 9 inches. This dimension was reduced to 5 inches in the model since the height of the model is only about 7 inches (Dsap4.pre13).

A summary of maximum stress in each of the 6 groups is tabulated in Table VI. Again these values represent only the stresses at the exposed surfaces of the mirror. The internal stress values are not being examined.

Table VI Maximum & minimum stress in each element group representing the stress value at the exposed surface of the detail model (with pad and hole)

group	max. (psi)		min. (psi)	
	computed	adjusted	computed	adjusted
1	153.	166.	-427.	-463.
2	168.	182.	-430.	-466.
3	60.	65.	-305.	-331.
4	63.	68.	-302.	-328.
5	116.	126.	-178.	-193.
6	123.	133.	-185.	-201.

A histogram showing the stress level distribution in this load case is illustrated in Figure 8. The maximum and minimum principal stress from this computation are:

max. principal stress = 182 psi
min. principal stress = -466 psi (8)

Stress with one of the 66 supports asserting a 250 lb. force

In normal operation, the mirror has 66 axial supports to support it's own weight. They also are able to assert a certain force pattern to the mirror to correct distortions caused by thermal and gravity effects. At each support the force range has an upper (or lower) limit of 250 pounds. This study is to determine whether this maximum force will produce an excessive stress level on the mirror.

The analysis started with the global model, with 65 supports held in position and a 250-lb. force applied to one support location. From the result the boundary conditions were established. They are transferred to the local model (with invar pad and hole in one rib) and more detailed intermediate boundary conditions are established. The maximum and minimum principal stresses are then determined by the local model analysis and results are summarized in Table VII. Again, the stress values are representing those at the exposed surface of the glass. Stresses within the glass are not considered relevant in this study. Data from both Table VII and the histogram shown in Figure 9 indicate that the majority of stress level is below 50 psi. The maximum and minimum principal stresses are:

max. principal stress = 32 psi
min. principal stress = -79 psi (9)

The maximum principal stress in the vicinity of the through hole is 27 psi., the minimum principal stress is -46 psi. Both are considered low in level. It can be concluded that the stress level in the vicinity of the through hole on the rib is not a major concern.

Table VII. Maximum stress in each finite element group of the local model when one of the supports is subjected to a max. force of 250 lbs.

group	tension(psi)	compression(psi)
1	32.	-79.
2	31.	-79.
3	15.	-55.
4	15.	-54.
5	24.	-30.
6	23.	-57.
11	27.	-46.

In this load case study, the force was applied towards the mirror. In real situations the force can be applied either in push or pull. Therefore the absolute stress values are more relevant in this case.

It should be noted that the gravity effect due to this 66-pt. support system was not being studied here. The assumption is that the stress value should be low in comparison to that of a 3-pt. support system.

During the analysis of the global model (Dsap4.6601) a 500 pound force was applied to the mirror. Correspondently, a 500 pounds force was also applied at the invar pad in the analysis of the local model (Dsap4.pre20). In the subsequent evaluation, all the computed values are halved in order to represent the true case.

Discussion

The maximum stress value for Ohara's E-6 borosilicate glass has not been determined. Particularly, in considering crack propagation in the surface of glass, the allowable limit is not entirely known. A practical limit of 5 N/mm sq (725 psi) was recommended by Schott for the Zerodur, and 7 N/mm sq (1015 psi) was recommended by Corning for the silica [3]. A limit as shown in eq. (10) is suggested for use as a reference.

Suggested limit for principal stress : 725 psi (10)

Noted that the positive value in (10) implies the limit is for tensional stress. The compressive stress is considerably higher. A comparison of results from this study is summarized in Table VIII :

Table VIII. A summary of maximum and minimum principal stresses from this study

case studied	tension(psi)	compression(psi)	safety margin
3 pt. support : gravity effect	182.	-466.	4.0
66-pt. support : 250. lbs force	32.	-79.	9.2

The local model is, no doubt, a better tool to determine regional detailed stress distribution. It can be testified by the values of principal stress in Table IX. It demonstrates that a misleading conclusion can be made if an inappropriate model is used. The global model shows that the highest stress is located at the rib above the support. In fact, the numerical values are in good agreement with those from the local detailed model to about 30%. (In tension, the global model yielded 50 psi, whereas the local model 68 psi. In compression, the global model yielded 278 psi, and the local model 331 psi.) Yet the global model is not able to pin-point the stress concentration at the back plate of the support. The local model indicated that the max. and min. stresses are 182 and -466 psi, whereas from the global model, the numbers are only 20 and -63 psi.

Table IX. A comparison of max. & min. principal stresses between global and local models

	global model		detail model	
location	tension(psi)	compression(psi)	tension(psi)	compression(psi)
rib	50	-278	68	-331
back plate	20	-63	182	-466

References

[1] Ray, F., and Chung, Y.T., "Analysis of a 7.6m Lightweight Mirror Design," McDonald Observatory, University of Texas at Austin, December 1984.

[2] Pearson, E., Stepp, L., and Keppel, W., "Support of 8-m borosilicate glass mirrors," Proc. of ESO Conference on Very Large Telescopes and Their Instrumentation, Garching, March 21-24, 1988, (M.-H. Ulrich, ed.), pp. 435-449.

[3] ESO, "VLT Proposal," report no. 57, March 1987.

[4] Soosaar, K., et. al., "Analysis and Trade-Off Studies of Large Lightweight Mirror Studies," The Charles Stark Draper Laboratory, Inc.. April 1975.

[5] Mack, B., and Harman, D.J., "Update on the 18m Aperture Multi-mirror Telescope Concept," IAU Colloquium No. 79, April 1984.

[6] Keppel, W., "Analysis of 3.5-meter Support System," Internal report, 1989.

[7] Bathe, K., Wilson, E., and Peterson, F., "SAP-IV, A structural analysis program for static and dynamic response of linear systems," College of Engineering, University of California, Berkeley, Calif.

Appendix

Appendix A - Fortran code for node and type-7 generation

Appendix B - Element numbering directory

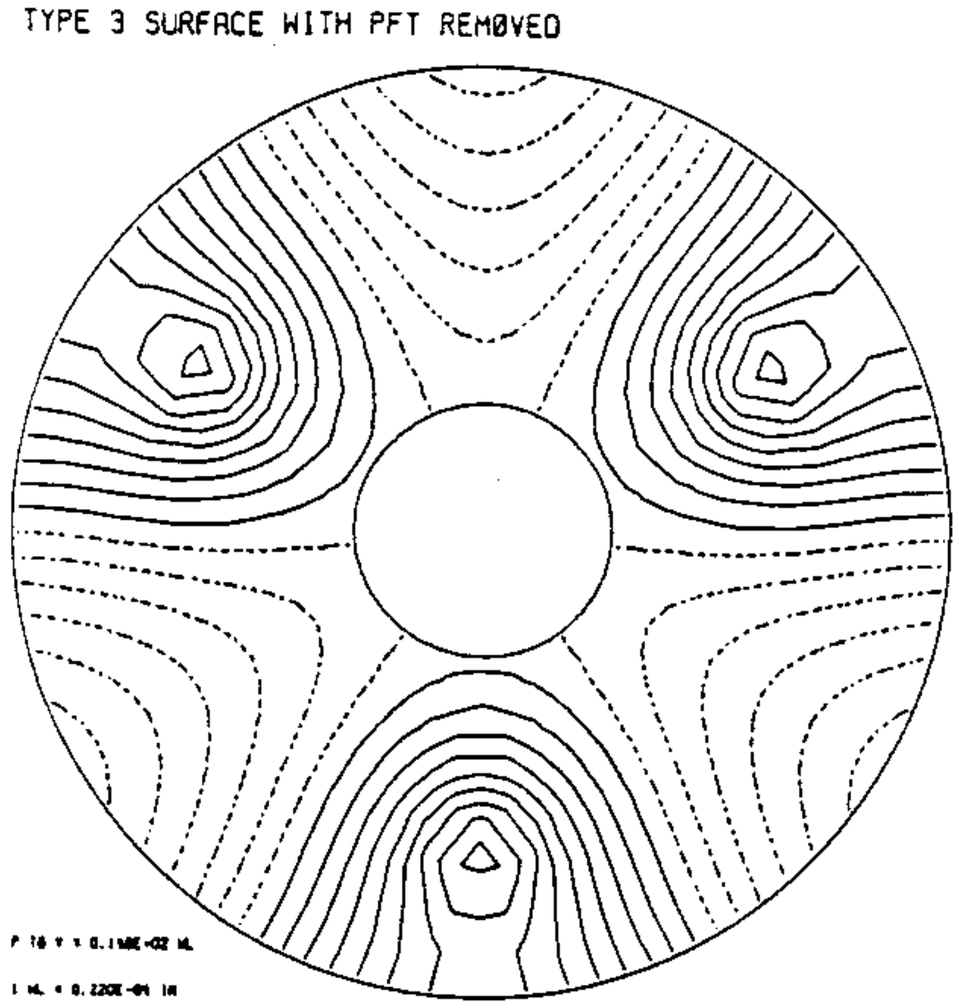

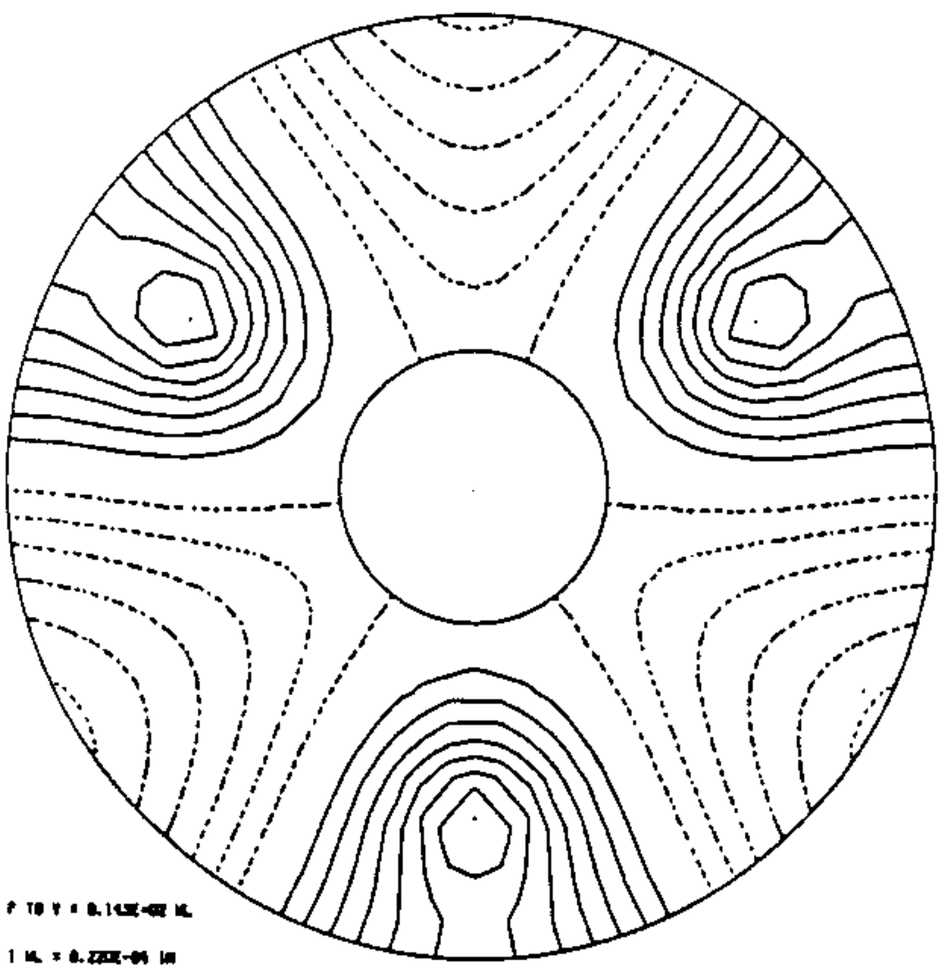

Figure 2. The self-weight surface distortions with a 3-point support system predicted by two different analytical approaches. (a) Using type-3 elements in which bending stiffness is not taken into account. (b) Using type-6 elements in which bending stiffness is included. The similarity between these two contour maps indicates the bending effect is not a significant factor to this particular loading condition.

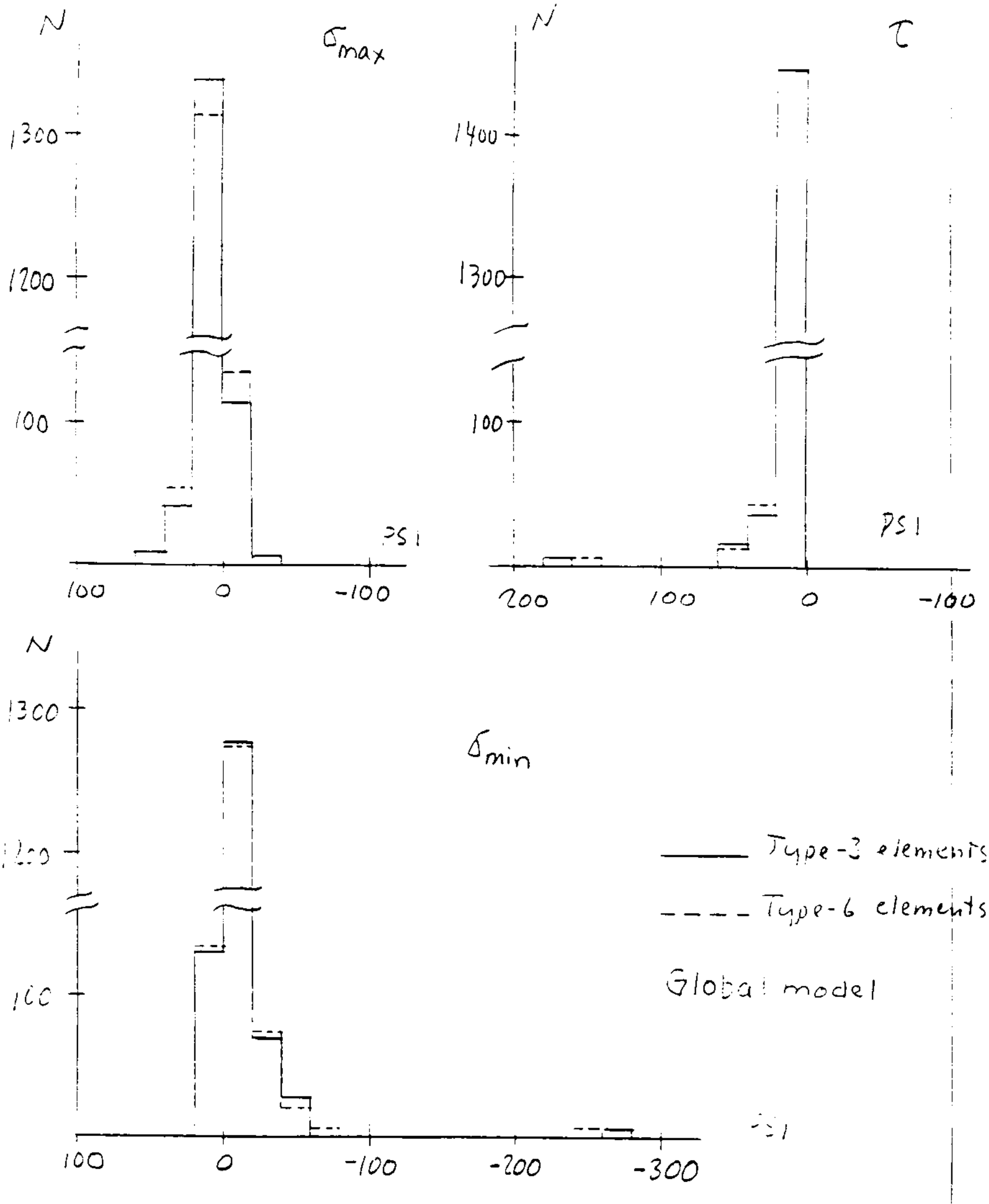

Figure 3. Histogram showing the distribution of max., min. and shear stresses using type-6 (with bending stiffness, in dashed line) and type-3 (without bending stiffness, in solid line) elements. The similarity of these two results is another indication that the bending stiffness is not a major factor affecting the stress value in this load case, namely, gravity stress with mirror supported at three points.

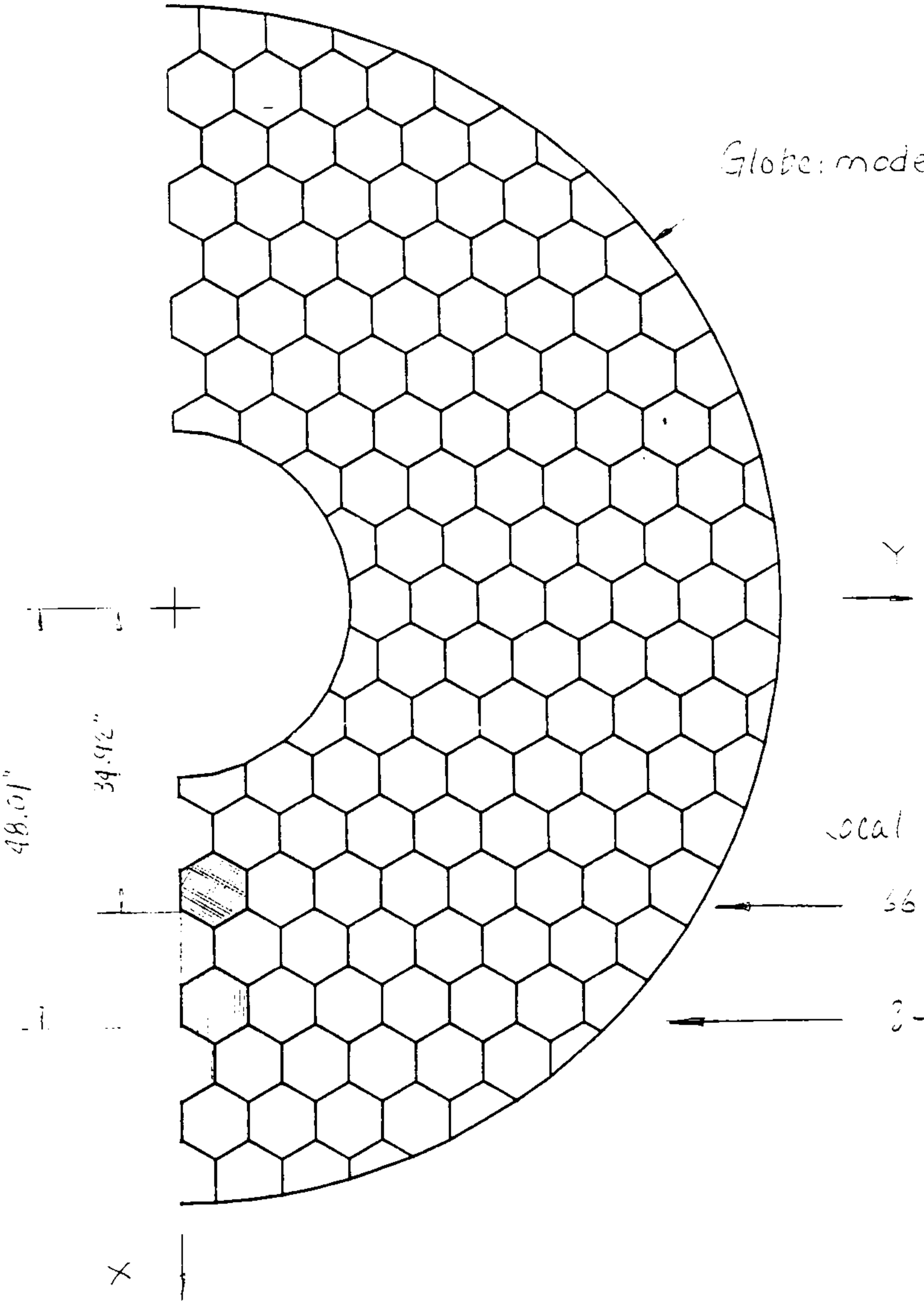

Figure 4. The outlines of the three models used in this study. The global model contains half of the mirror. Two local models cover the lower part of one and one-half mirror cells. One local model is for the 3-support case, and the other the 66-support case. The analysis of the global model provides an overall stress distribution of the mirror. The analyses of the two local models provide a detailed stress distribution in the vicinity of the mirror supports.

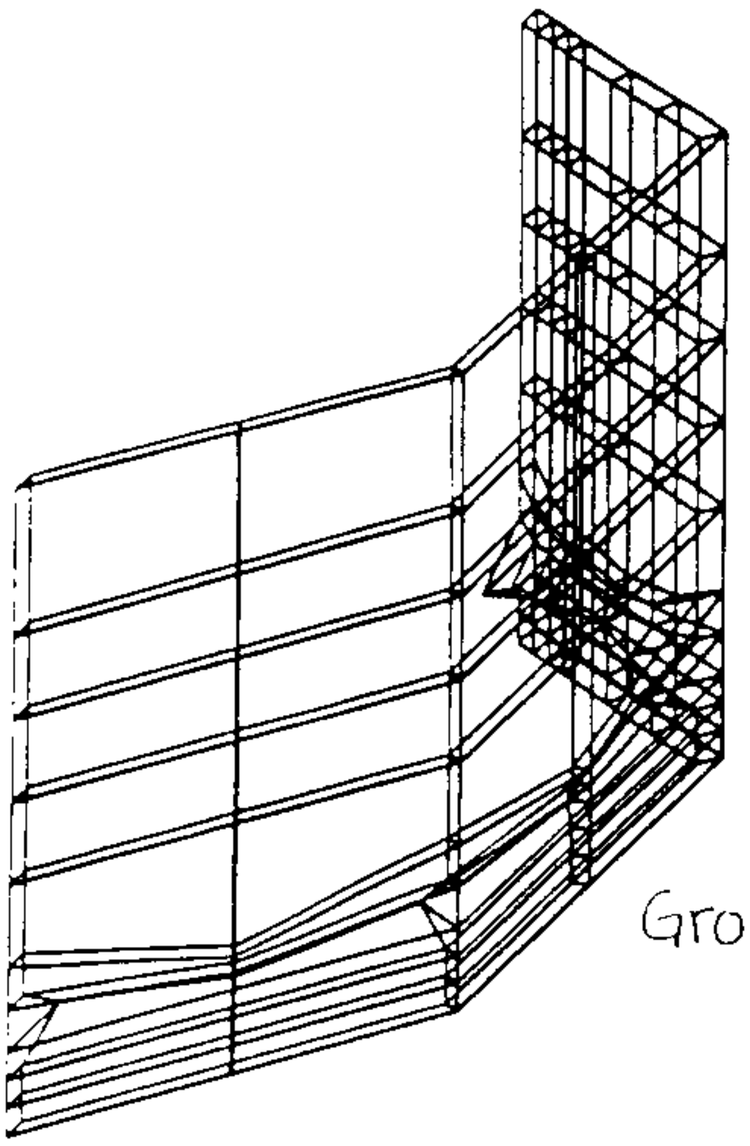

Group 3

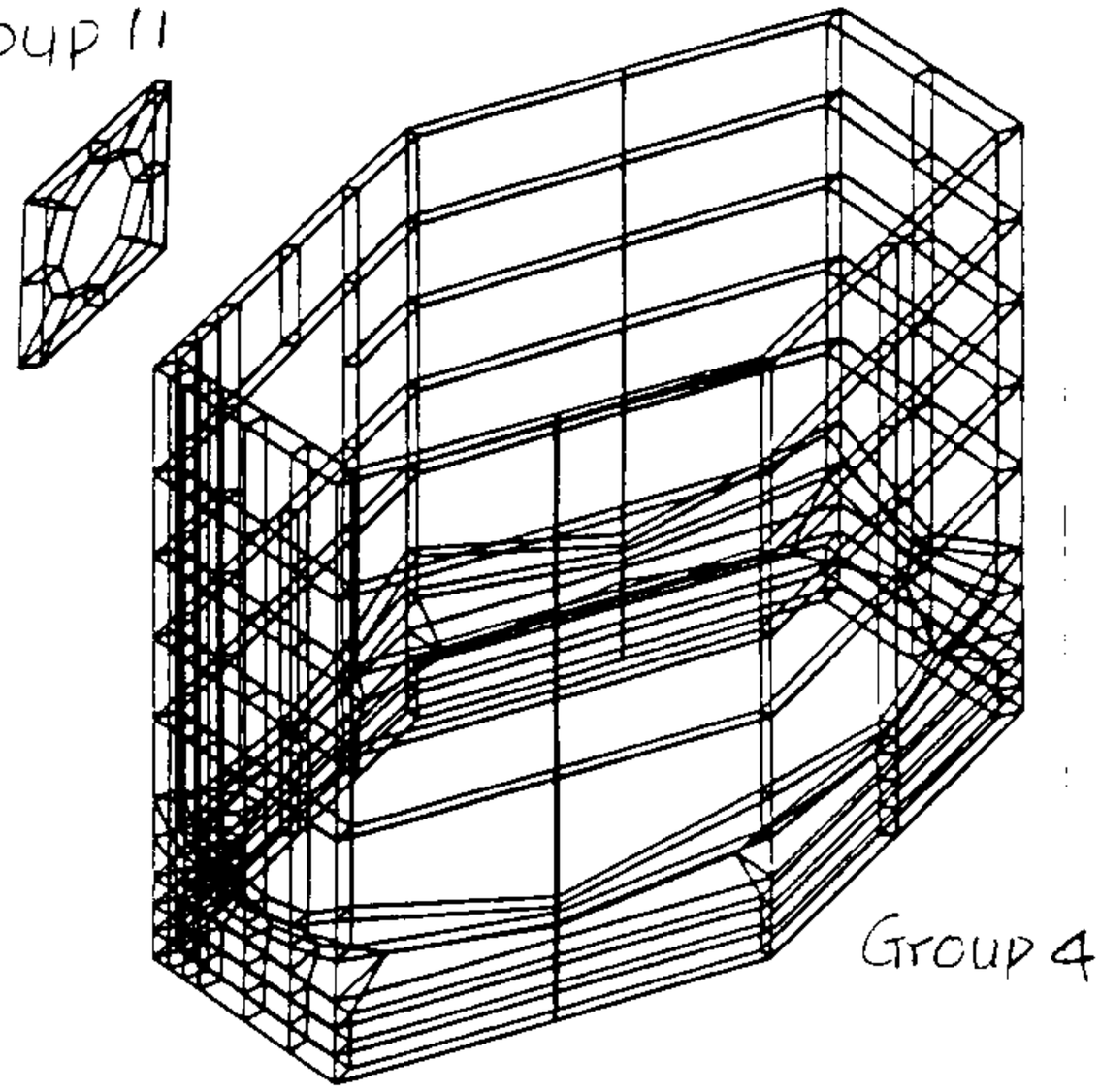

Group 4

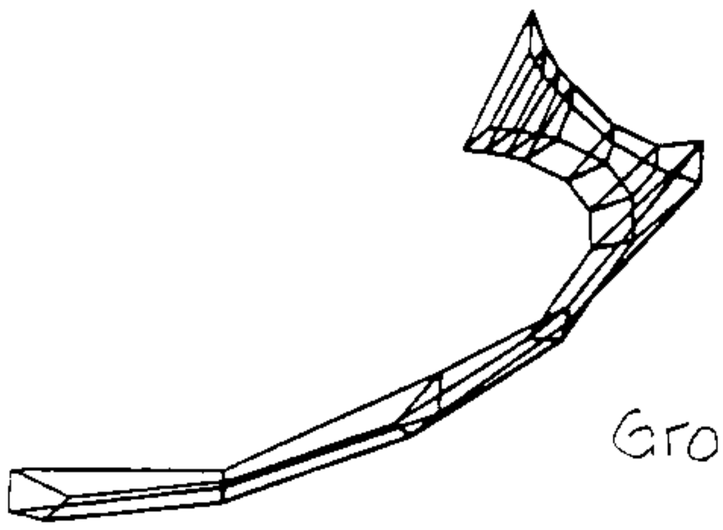

Group 5

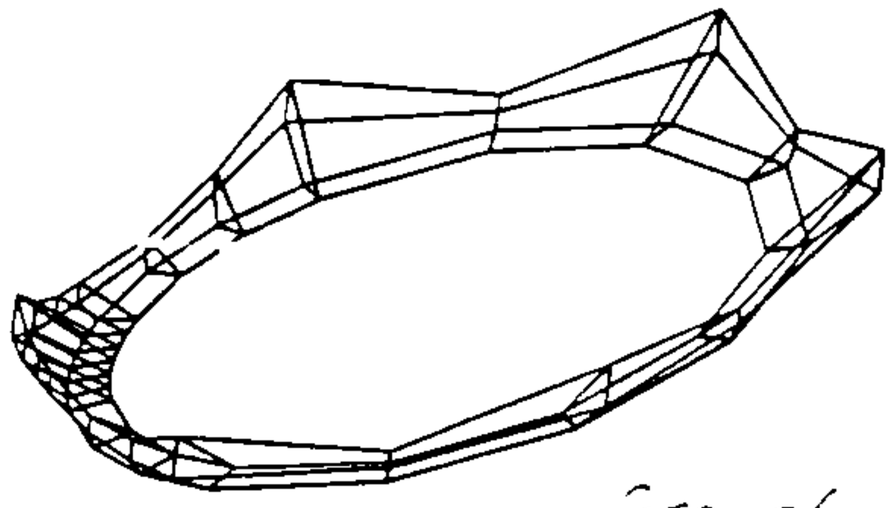

Group 6

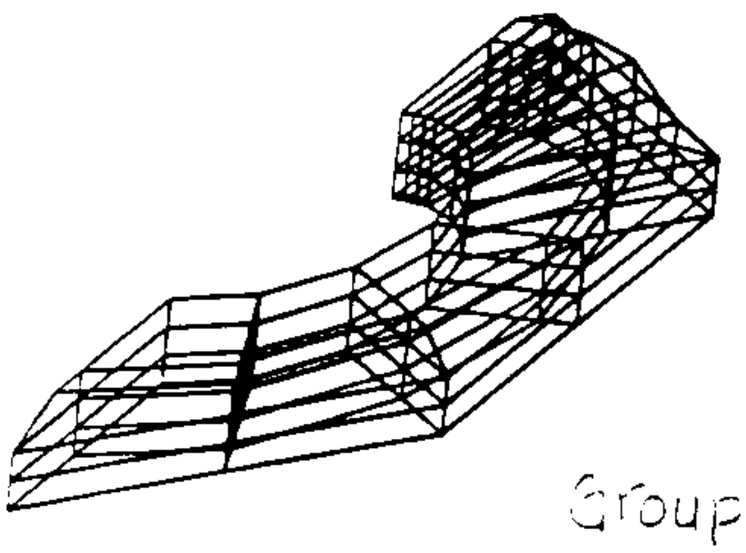

Group 1

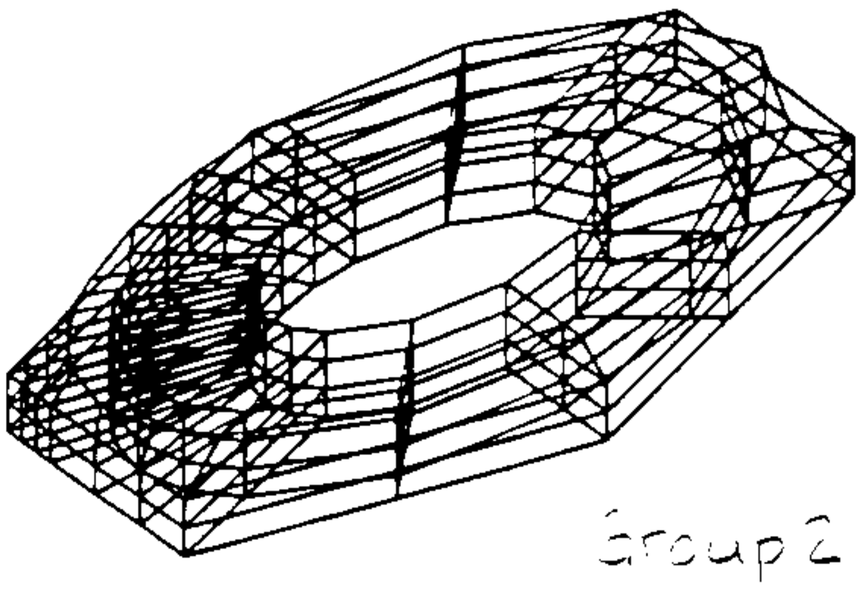

Group 2

Figure 5. The outline drawings showing the type-5 brick elements used in the local models. They represent the lower part of the mirror in detailed form. Groups 1 and 2 represent the back plates; groups 3 and 4 the ribs; groups 5 and 6 the filets, and group 11 the hole on one rib.

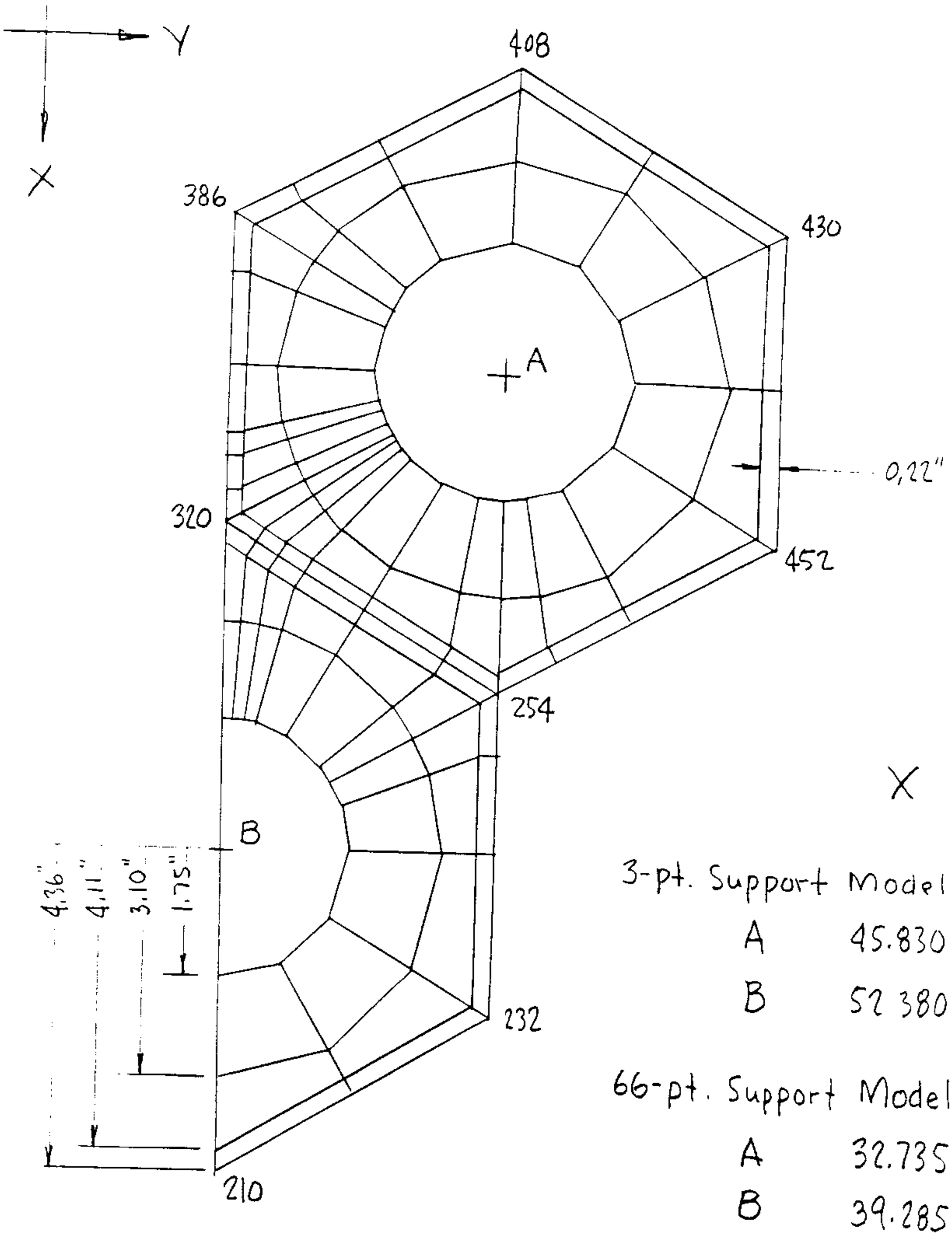

Figure 6. Relevant input parameters used to generate nodes for the local model. Three programs are written for this purpose. The listing of these programs are included in Appendix A.

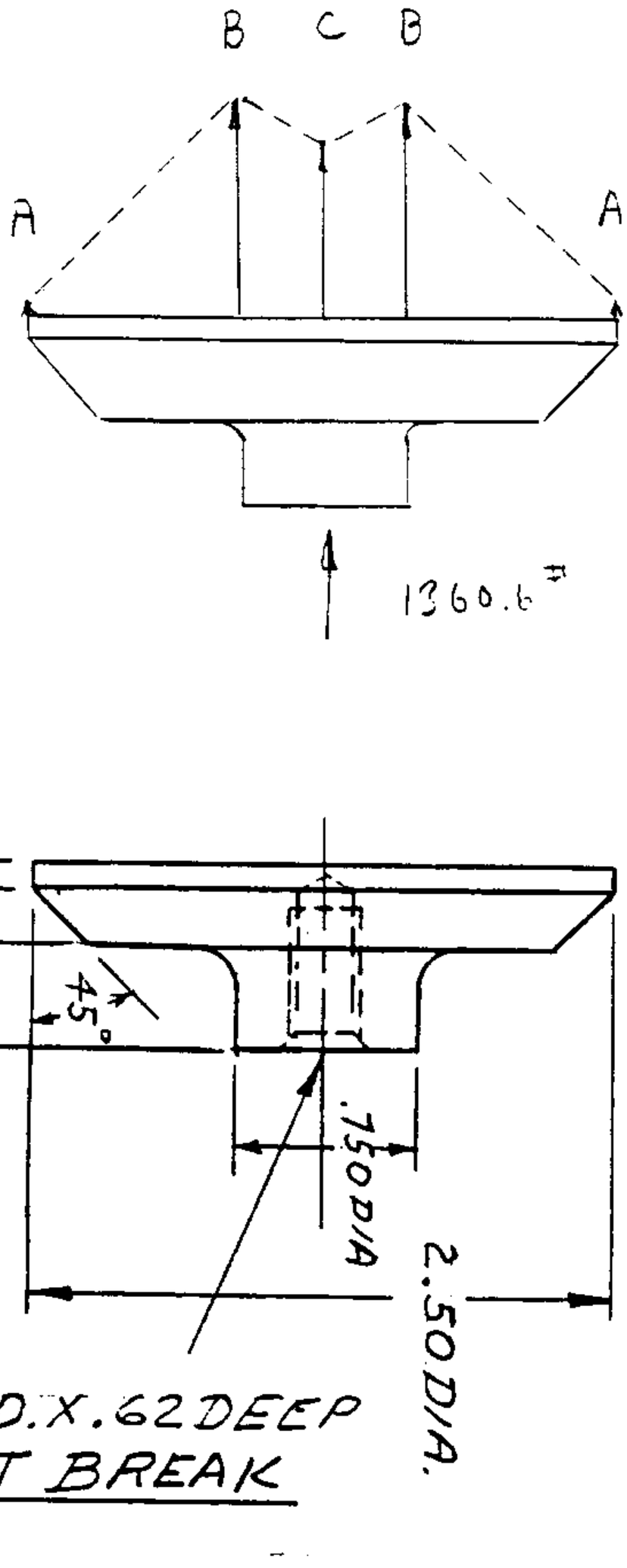

Force Vector n

A = 6# 24

B = 95# 12

C = 77# 1

T = 1361#

(a)

(b)

Figure 7. The mirror support pad made of invar. (a) The applied force and the reaction. (b) An engineering drawing by R. Harris.

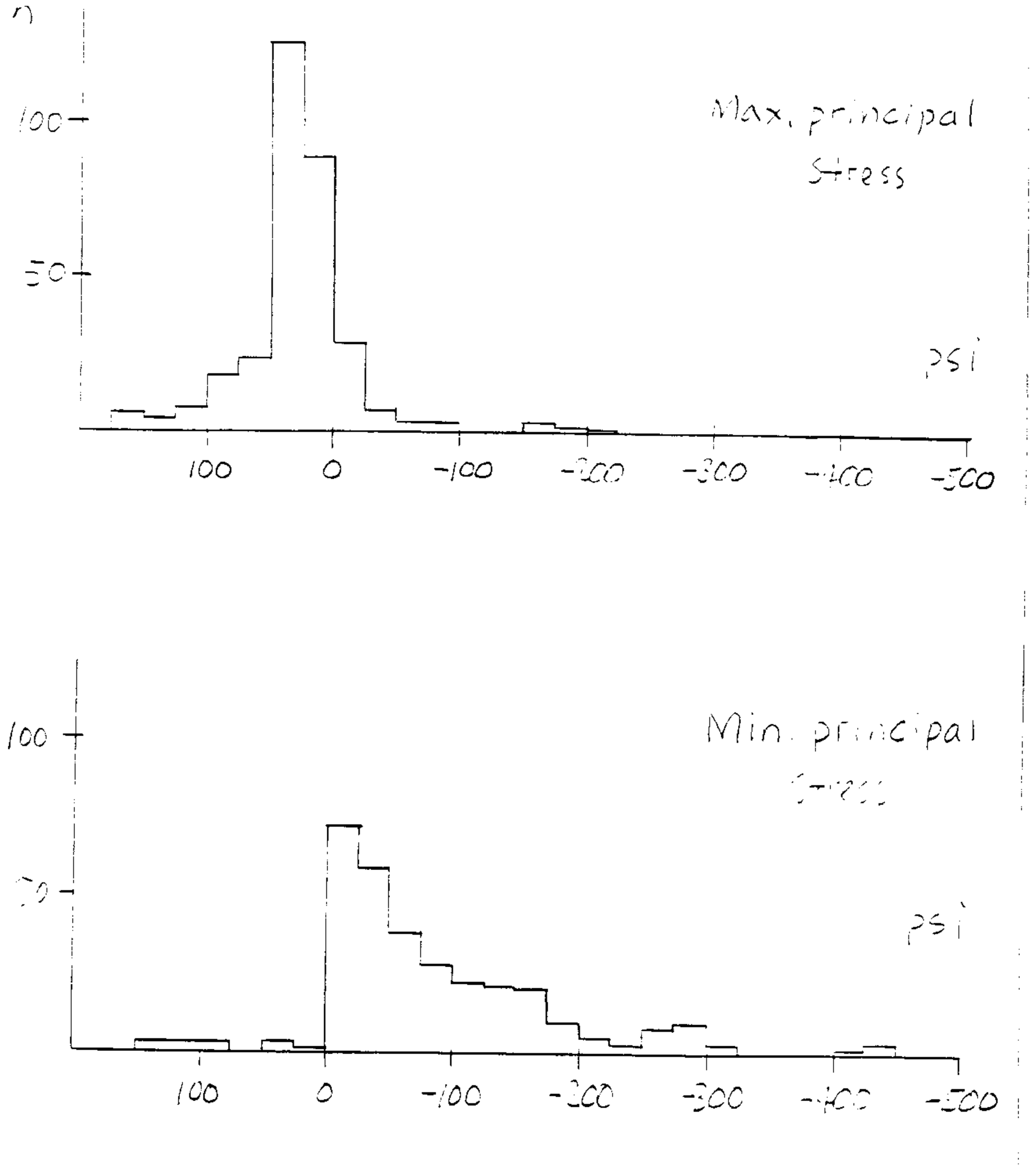

Figure 8. Histogram showing the max. and min. stress distribution in the local model. The stresses are caused by the mirror's own weight when supported at three points. The max. principal stress is found to be 182 psi, and the min. principal stress -466 psi.

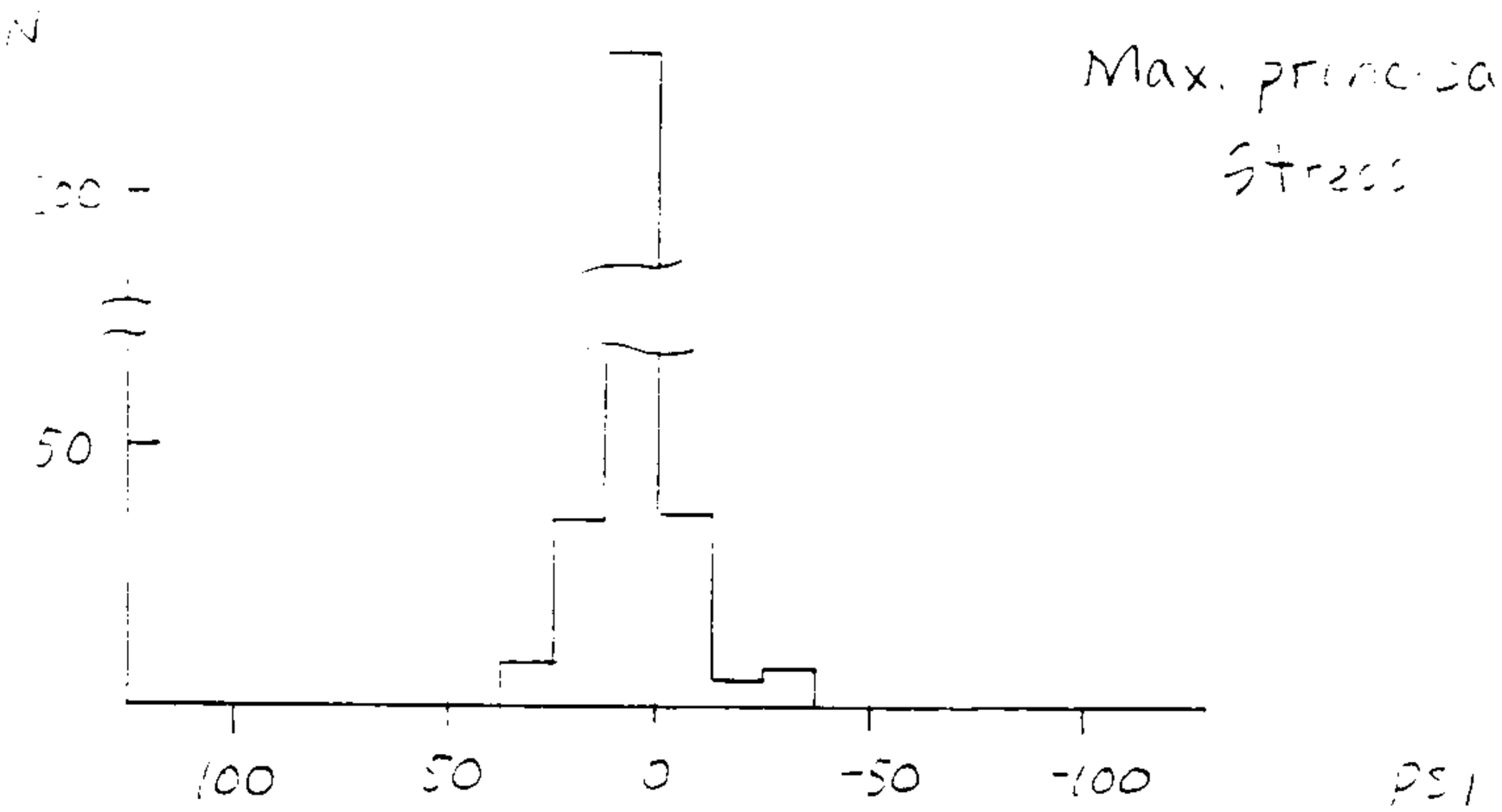

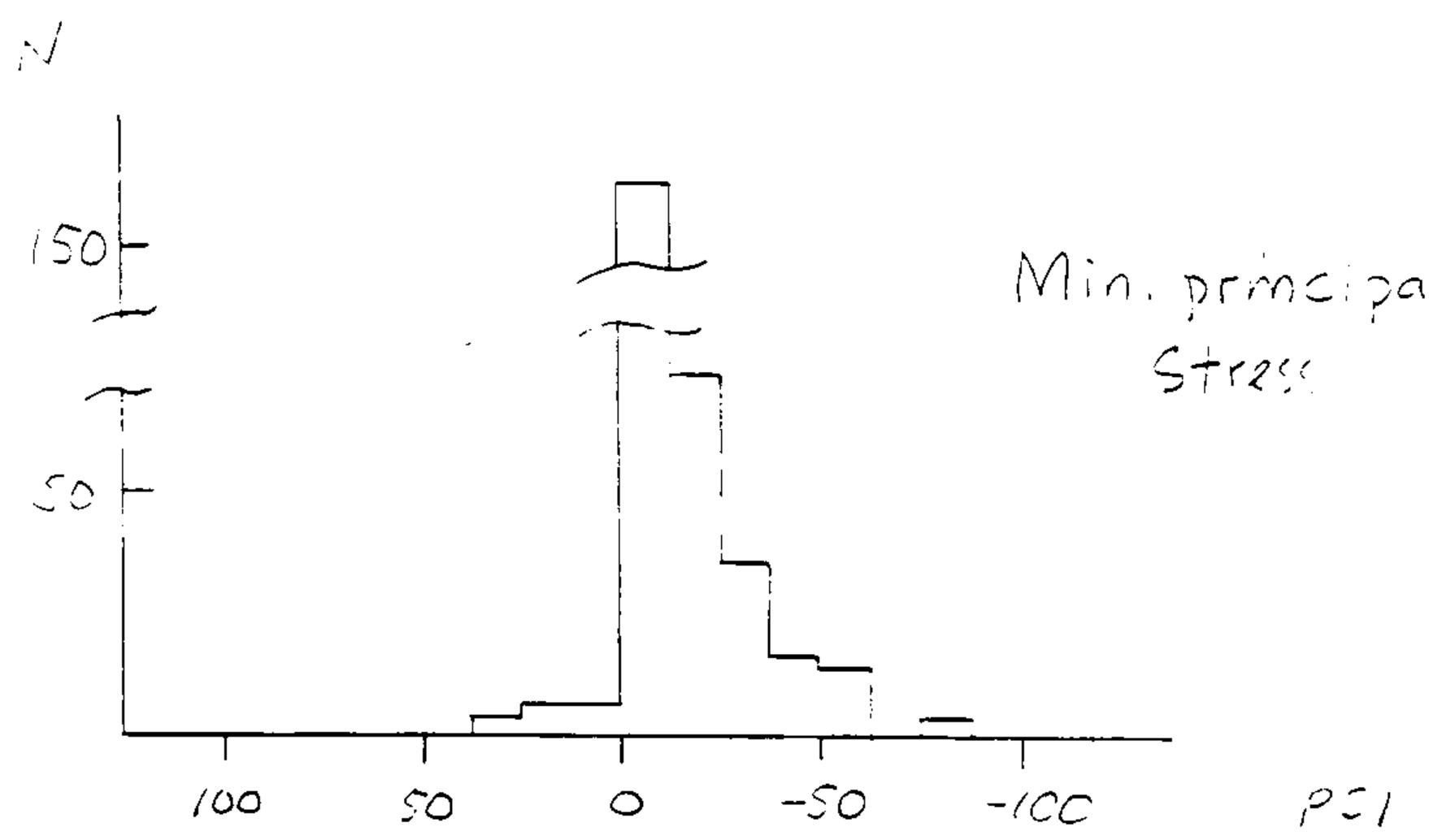

Figure 9. Histogram showing the max. and min. principal stresses in the local model caused by a 250-lbs. force applied toward the mirror at one support location with the rest of the 65 supports held in position. The max. stress is found to be 32 psi, and the min. stress -79 psi. Since the force can be applied in either direction, one should consider the absolute value in this case. Therefore the value of 79 psi is the max. stress.